Karol Brzeziński
Dr inż.
Zakład Mostów i Dróg Szynowych,
Wydział Inżynierii Lądowej
Politechniki Warszawskiej
k.brzezinski@il.pw.edu.pl

Rafał Michalczyk
Dr inż.
Zakład Mechaniki Teoretycznej i Mechaniki
Nawierzchni Komunikacyjnych, Wydział
Inżynierii Lądowej Politechniki Warszawskiej
r.michalczyk@il.pw.edu.pl

DOI: 10.35117/A_ENG_19_05_01

Changing the dynamic characteristics of the track to reduce noise emissions - numerical study

Abstract: The paper presents the concept and preliminary results of numerical study of changes in the rail track dynamic characteristics. Change of the characteristics is introduced in order to reduce noise emissions. The theoretical relationship between the studied track dynamic characteristics (TDR - Track Decay Rate) and noise was briefly explained, and then the methodology of FEM modelling for the standard test simulation was described. Four mass modification variants and two rail types (49E1 and 60E1 profiles) were analyzed. Numerical study show correlation between the railroad track mass increase and its dynamic characteristics and thus the noise emission. It turns out that the obtained effect may cause reduction of noise emission in some frequencies, and increase in others.

Keywords: Track decay rate; Track dynamics; Rail dampers; Noise reduction; FEM

Introduction

Rail transport is a source of significant noise and vibrations - mainly due to mechanical vibrations, and to a lesser extent the impact of air resistance. The reduction of these adverse effects without significant financial outlays and excessive complications in the construction and operation of railways should go hand in hand with the development of railway infrastructure. The key to achieving this goal is to understand the sources of noise and vibration and the parameters that may affect them, and then propose economically sound technical solutions.There are many studies devoted to the theoretical description of phenomena that make up the noise associated with rail transport [10]. The noise during the passage of the rail vehicle may be a mixture of rolling noise, aerodynamic noise and others.

Research conducted for years indicates that in many situations rolling noise is the dominant source of sound (see [5, 6, 1]). It is generated by the roughness or waviness of the surface of the wheel and rail, which causes dynamic forces affecting the contact surface. As a consequence, this results in relative vibrations of the wheel and rail, wherein the amplitude of the vibrations of each element depends on its dynamic properties. The vibrations created in this way are the main source of noise.

There are developed analytical and empirical models for predicting the intensity of the sound emitted for particular types of wheel and track depending on the roughness. The TWINS model (Track Wheel Interaction Noise Software) [7] is the most widely used, thanks to which rolling noise can be calculated as the sum of the sound power emitted from the

wheel, rail and underlay. The condition is to have the results of measurements carried out on an existing track and thus virtual testing of new solutions is limited.

The dynamic properties of the railway track are crucial in noise forecasting, and the appropriate track dynamics model should take into account interactions between different components [13]. The rail can be treated as an infinitely long beam in which the propagation of mechanical waves takes place. In addition, the rail has much more damping capabilities than the wheel due to its attachment. This damping is mainly due to energy losses during transmission of a mechanical wave from the load point along its length. The speed of decay of these waves along with the distance along the rail determines the so-called effective length of the rail. For this reason, the attenuation introduced by attaching to the sleepers is an important parameter for the track, because it affects the disappearance of vibrations along the track, and thus determines the effective length that is subject to vibrations. The longer the rail section, which vibrates under the influence of each wheel, the more noise will be emitted. We can distinguish three main sources of this damping: losses occurring in fastening systems (e.g. rail pads), energy transferred to sleepers and embankment, and damping of the rail [8]. Support systems block transmission of vibrations along the rail but only at low frequencies. On the other hand, the transfer of vibrations to the sleepers and embankment (application of rigid supports) causes that the sleepers themselves become the source of noise, and the vibrations have an adverse effect on objects located near the railway line. Increasing the ability of the rail itself to damp vibrations seems to be the best solution.

The amplitude of the rail vibrations decreases approximately exponentially along with the distance along the track. The more damping the path, the faster the loss of vibrations. The parameter used to describe this phenomenon is the decay rate of the vertical and transverse vibrations of the track (Track Decay Rate - TDR, comp. [3]) and the value is usually expressed in dB / m. The decay rate is the most important indicator of the dynamics of the track in relation to rolling noise. Low values of this parameter lead to a longer effective length of the rail, and thus to high noise emission from the track. High TDR values cause less noise and can be obtained, for example, by using rigid washers between the rail and the sleepers. However, soft pads are often used for non-acoustic reasons, e.g. to minimize damage to primers or vibrations transmitted through the ground. TDR values derived from measurements are commonly used to calculate rolling noise in models such as TWINS. According to the norm [2], the coefficient can be determined experimentally, using a hammer/modal hammer and accelerometers. It is also possible, although technically more difficult, to determine the TDR coefficient by measuring the vibration of the rail during the passage of the train.

From the point of view of noise reduction, it is desirable to design such solutions that increase the TDR ratio while maintaining the insulation of the sleepers (without introducing stiffer rail pads). One of the more effective solutions are the tuned absorbers systems [12]. The theory of such a tuned arrangement of the rail and muffler is presented in [11].

The aim of the article is to present the methodology of forecasting the TDR coefficient depending on the dynamic characteristics of the track. Changing the characteristics can be achieved by using silencers. The initial verification of the solutions was made with the use of FEM computer simulations (finite element methods). The analysis was carried out in two stages. In the first stage, the entire track was modeled (one rail track, taking into account the elastic foundation on the sleepers and then the ballast). The results from the first stage analysis served as a reference point. In the second stage, the track was modeled along with a simplified model of the device (in the form of a discrete mass). The main goal is to develop a silencer that significantly increases the TDR coefficient and thus potentially the most effective solution in terms of noise attenuation.

The relationship between the TDR parameter and the noise emitted is described, among others in the annex to the standard [2]. The vibration amplitude of the rail course

decreases with the distance from the excitation point (which is actually the point of contact between the wheel and the rail, and during the TDR test the point of impact with a hammer). The measured value is usually the acceleration or speed of the rail running in the direction perpendicular to the track axis (vertical or horizontal). In figure **1**, this relationship is illustrated by taking the reference point at the point of being as a reference point.

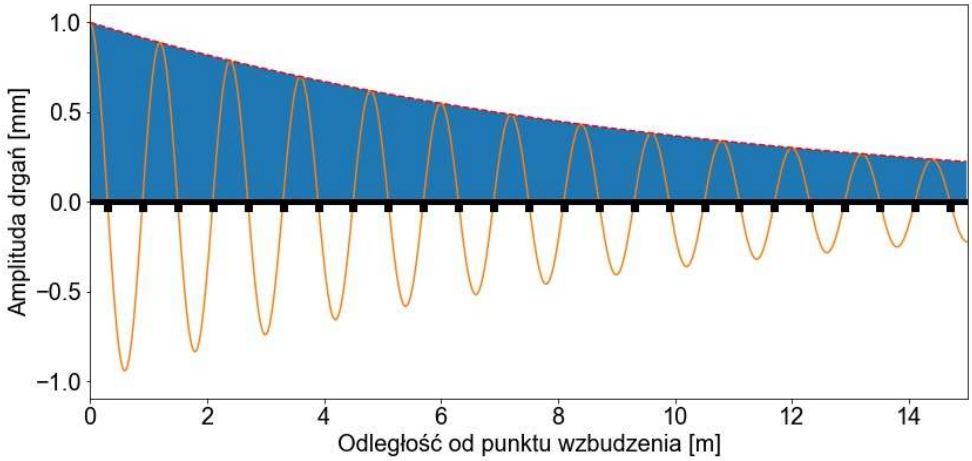

1. Loss of vibration amplitude along the track (dotted red line described by the formula 1)

Although the case of the classic ballast surface, the rail is supported periodically, which means that the function describing the disappearance of vibrations does not have to be monotonic. However, in practice, for the sake of simplicity, it is assumed that the amplitude of the vibrations changes according to the following dependency:

$$A(x) = A(0)e^{-\beta x} \tag{1}$$

where:
A – vibration amplitude (normal acceleration [m/s^2] or speed [m/s]),
x – distance from the excitation point [m],
β – parameter describing the speed of vibration decay [-].

The power of the sound emitted by the rail is proportional to the vibration amplitude along the rail course $\int_0^\infty |A(x)|^2 dx$. It also depends on other parameters (e.g. acoustic impedance of the air), which we cannot influence. On the other hand, the β parameter can be influenced by the use of appropriate structural solutions (e.g. pads, underlays), or additional devices (silencers). Therefore, it is used in the assessment of track dynamics and indirectly its acoustic properties. Theoretically, it can be determined on the basis of the slope of the vibration decay diagram (see equation 1), shown in the semi-logarithmic plane. However, due to the deviation of the actual results from the ideal exponential dependence, the standard [2] recommends the use of a simplified formula (the derivation of the formula can be found in the annex to the standard).

$$TDR \approx \frac{4{,}343}{\sum_{n=0}^{n_{max}} \frac{|A(x_0)|^2}{|A(x_n)|^2} \Delta x_n} \tag{2}$$

The field test, allowing to determine this parameter, is performed by measuring the acceleration signal (or speed) at different distances from the excitation point. For practical reasons, the geophone or accelerometer is mounted for the duration of the test in one cross-section. In contrast, the excitation location is variable (impact with a hammer, with a suitable tip to measure force). The distribution of points in the initial part of the study is shown in Figure **2**.

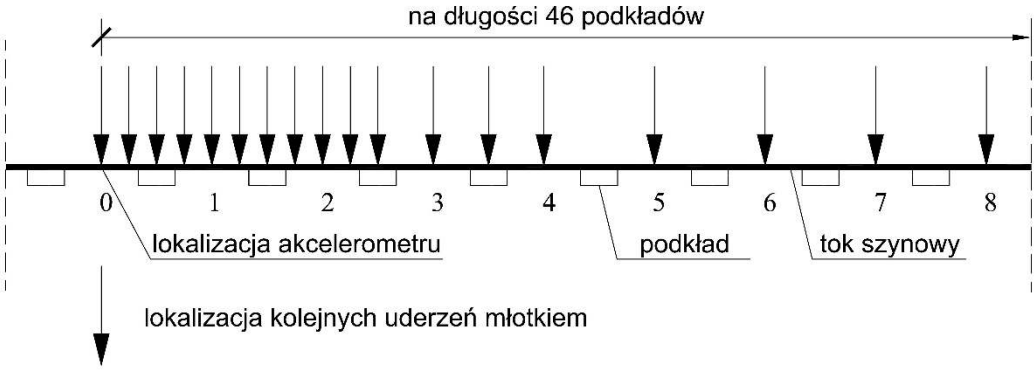

2. Schematic diagram of the TDR test

Research methodology

The analyzes are based on computer simulation using FEM (finite element methods). The simulation of the TDR test is carried out using the model shown in Figure **3**. At the current stage of the research, the dampers were replaced with masses focused rigidly connected to the rail tracks.

- Simulation of the TDR study was carried out in two stages:
- track without dampers,
- track with silencers in the form of a rigidly attached mass,

A more general model is shown in Figure **3**. The lack of dampers can be obtained by substituting the zero mass added in the model. The track without dampers is a reference point against which the proposed solutions will be evaluated. The model with rigidly clamped masses aims to assess to what extent the dynamic properties of the track depending on the mass of the silencer. So that in future studies it would be possible to compare results with more advanced models using viscoelastic characteristics (reflecting the rigidity of the casing and damping the properties of the material).

The TDR study was prepared in the Abaqus and Python environments. The model was parameterized, among others in terms of:

- length of the tested track section
- spacing of sleepers
- replacement weight of discrete silencer
- parameters of the rail pad
- ballast parameters
- impulse for vibration.

The model (Fig. **3**) enables testing using two different rail profiles (60E1 and 49E1). The acceleration signal is read at the points indicated by the standard [2].

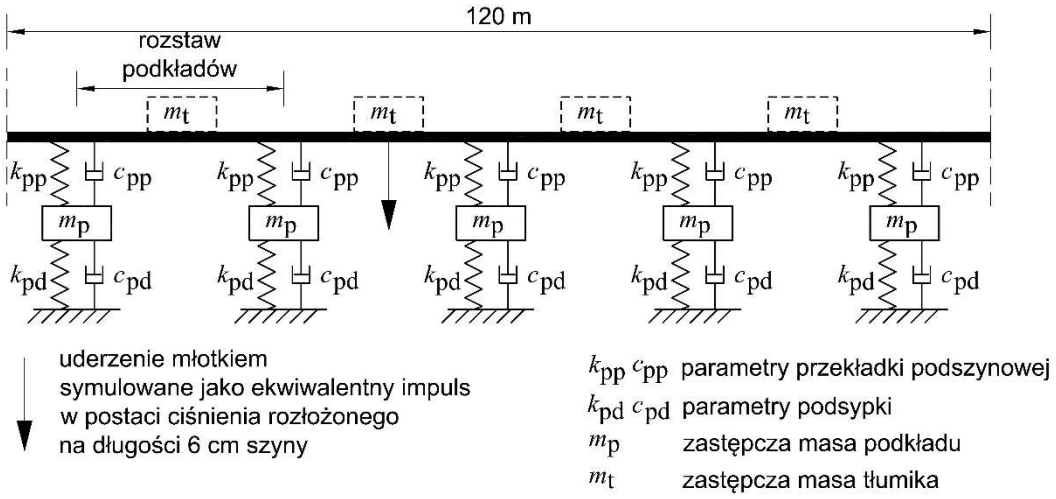

3. Substitute track model for simulating the TDR test

For all analyzes, the same track parameters were adopted. They were adopted mainly on the basis of the results of previous studies available in the literature [4, 9] and summarized in Table **1**.

Table **1**. List of adopted parameters of the track model

Parameter	Parameter value	Unit
length of the model (half)	60	m
substitute mass of foundations	150	kg
spacing of sleepers	0,6	m
elastic parameter of the under sleeper pad	$2{,}0 \cdot 10^8$	N/m
viscous parameter of the under sleeper pad	$1{,}0 \cdot 10^6$	N·s/m
elastic parameter of the ballast	$5{,}0 \cdot 10^7$	N/m
sticky balast parameter	$1{,}0 \cdot 10^5$	N·s/m

Using the above-defined model, a series of analyses were carried out, assuming various masses of silencers (substitute mass corresponds to two silencers located on both sides of the rail):

- variant No. 0 - mass m_t = 0 kg
- variant No. 1 - mass m_t = 6 kg, which corresponds to 10 kilograms per meter of rail,
- variant No. 2 - mass m_t = 12 kg, which corresponds to 20 kilograms per meter of rail,
- variant No. 3 - mass m_t = 18 kg, which corresponds to 30 kilograms per meter of rail,

FEA analysis was carried out in the Abaqus® environment. The entire system was modeled in 2D space. The rail pulley was modeled with a continuous beam. Discrete visco-elastic joints (rails with sleepers and foundations with the ground) were created using special elements designed for this purpose (so-called *engineering features*). A linear load was assumed in the form of a rectangular pulse, distributed evenly over a distance of 6 cm in the middle of the span. The duration of the pulse is 0.0023 s and its amplitude is $2.775 \cdot 10^6$ N / m, which is supposed to simulate a hammer blow during the standard TDR test.

The beam has been divided into 15 cm finite elements with square shape functions. The model reproduces a fragment of a track with a length of 120 m. However, because the symmetry conditions have been used, the length of the model is 60 m.

The dynamic analysis was carried out in two steps (standard type - implicit). The first step is the load phase lasting 0.0023 seconds. The second step is represented by free vibrations in the time of 0.20 s. A constant increase of time in the following analysis periods was assumed, which was $8.0 \cdot 10^{-5}$ s, allowing recording of vibrations with a frequency of 5000 Hz. After the calculation, an acceleration signal recorded at the nodes was recorded in the same distance as during the standard test [2]. Visualization of the track model (without dampers) with marked points on the initial section of the track is shown in Figure **4**.

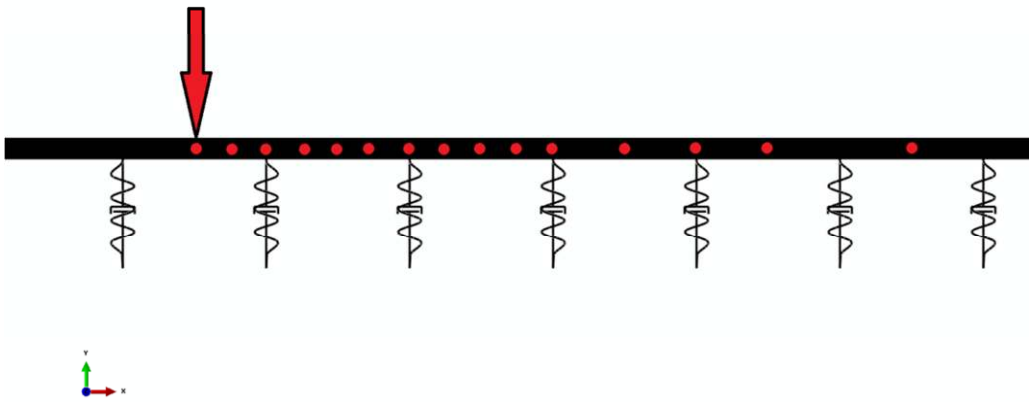

4. Location of measuring points on the initial section of the track

The acceleration results were processed using the Python environment to visualize and analyze the impact of the applied dampers on the dynamics of the track. The acceleration signal from each point is band-filtered to split into 1/3 octave bands from 100 to 5000 Hz. A Butterworth filter was used for this purpose, determined by the function of transmittance:

$$H(f) = \frac{1}{\sqrt{1+\left(\frac{f}{f_0}\right)^{2n}}} \tag{3}$$

where:
f – filtered frequency [Hz],
f_0 – cut-off frequency [Hz],
n – filter row (adopted $n = 4$) [-],

Then, the mean square of the RMS (root mean square) signal is calculated from each sample. It is an estimation of the amplitude, because, with the assumption of signal harmonics, the amplitude is proportional to RMS. The assumption is a significant simplification, however, used in practice.]

On the basis of each set of samples from all measuring points and a given third-octave band, the TDR value is calculated according to equation 2. The results of all measurements are presented as a function of frequency. Increasing the TDR at a given frequency can be interpreted as a reduction in the noise emitted. The application of a given solution may cause an increase in TDR in one frequency range and a decrease in another. Therefore, in order to compare two solutions, one should still adopt the optimization criterion. The procedure for analyzing the results is shown schematically in Figure **5**.

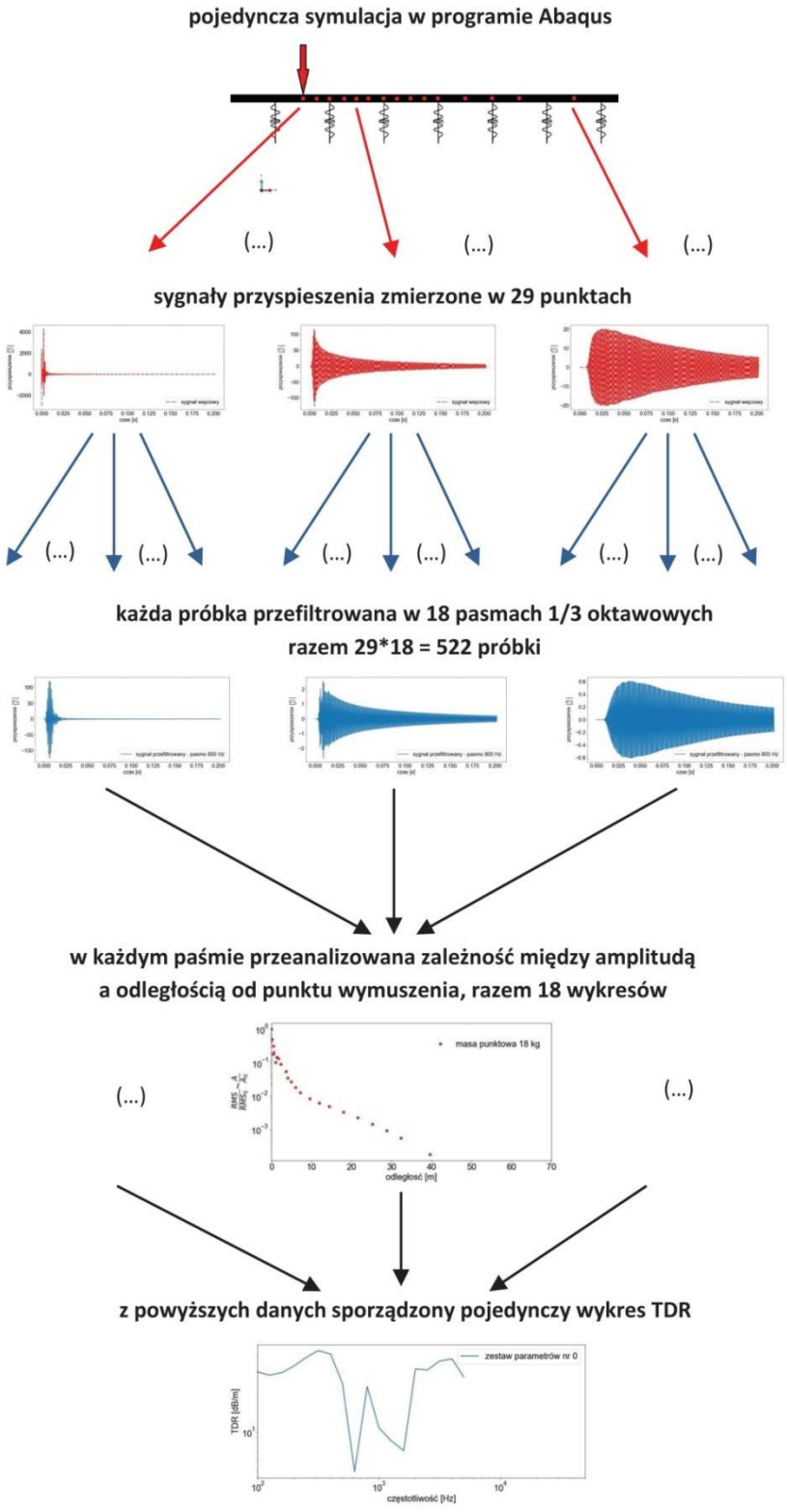

5. Processing diagram for calculating TDR based on the results of FEM simulation

Analysis of results

According to the adopted methodology, first of all signals of accelerations at measuring points along the rail course were determined. However, in order to verify the correctness of the conducted simulations, especially at the initial stage, other aspects of the dynamic response of the structure (e.g. displacement) were also analyzed. The visualization of displacements recorded in the final stage of load application is shown in Figure **6**.

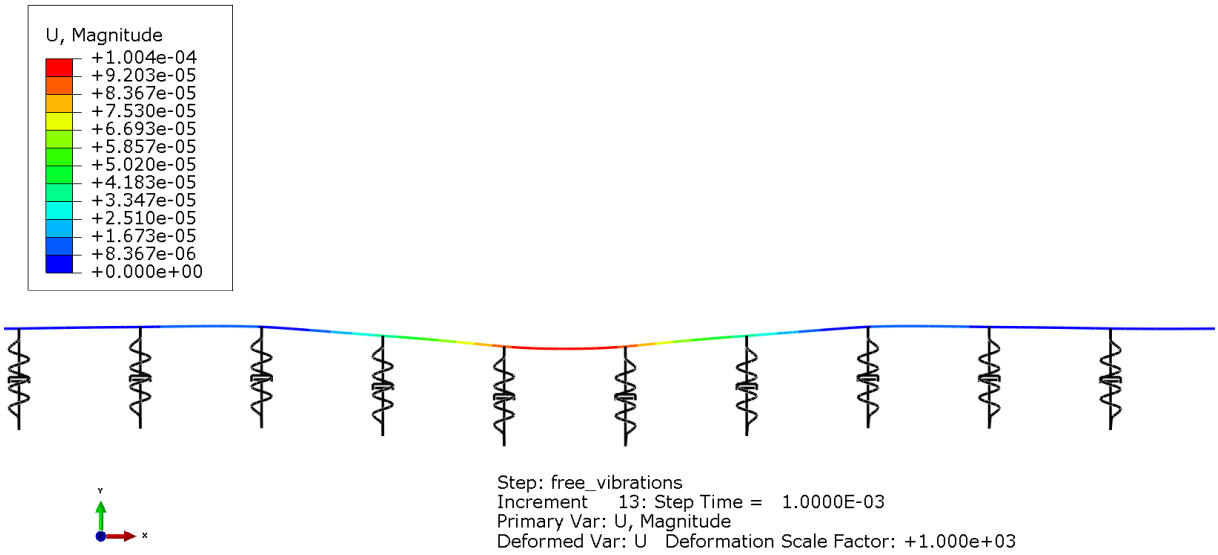

6. Deflection of the rail coupling in the final phase of the load (scaled 103 times) - maximum deflection 0.11 mm

The track decay rate, which was used to assess the effectiveness of solutions is highly processed and aggregated information, which can be seen in the scheme of conduct (Figure **5**). Before starting to calculate the TDR track, the output and intermediate calculation results were analyzed. Selected results will be presented and discussed below. In the case of acceleration graphs with a green background, the analysis step is marked, in which the loads are applied and the white vibrations are free.

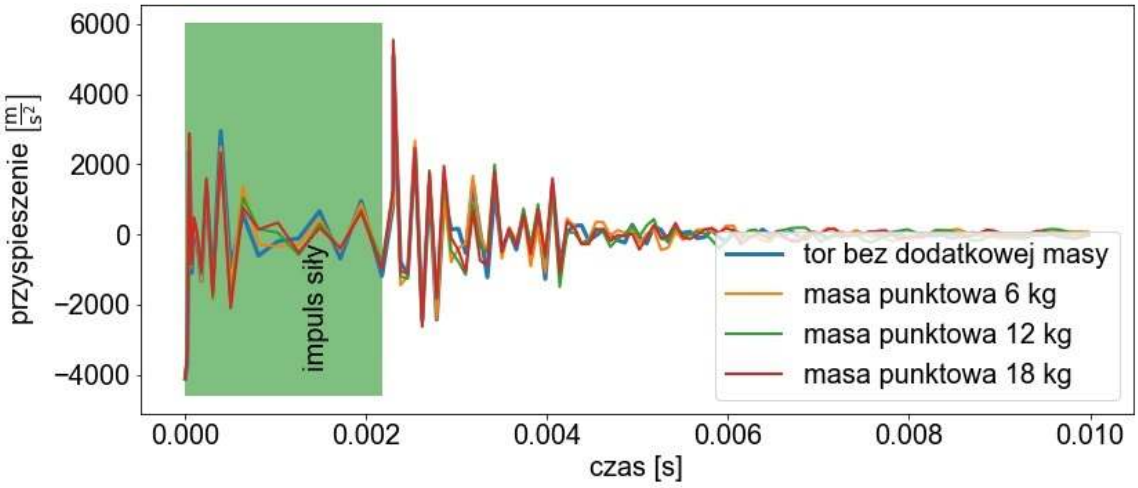

7. Acceleration signal registered at the point of load application. Track with 49E1 rail profile

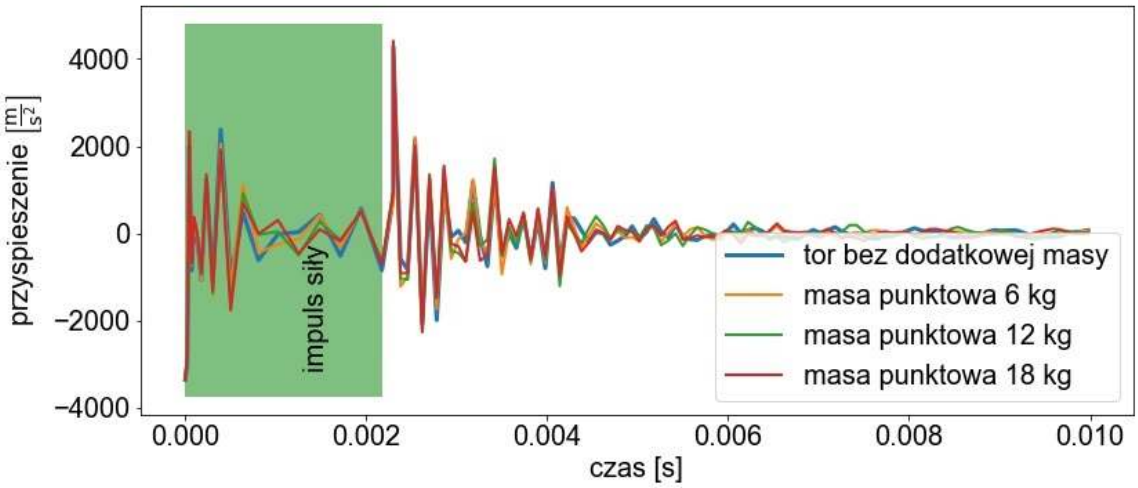

8. Acceleration signal registered at the point of load application. Track with rail profile 60E1

Figures **7** and **8** present the acceleration signals recorded at the point of load application, respectively, with the use of rail profiles 49E1 and 60E1 in the track. Acceleration graphs are very similar, regardless of the use of additional mass. The comparison of results between the 49E1 and 60E1 profiles also allows us to state that the nature of the acceleration does not differ significantly in the case of both profiles. However, as for the maximum values, it can be seen that the acceleration amplitudes are greater in the case of the 49E1 profile, which is, of course, related to its lower stiffness.

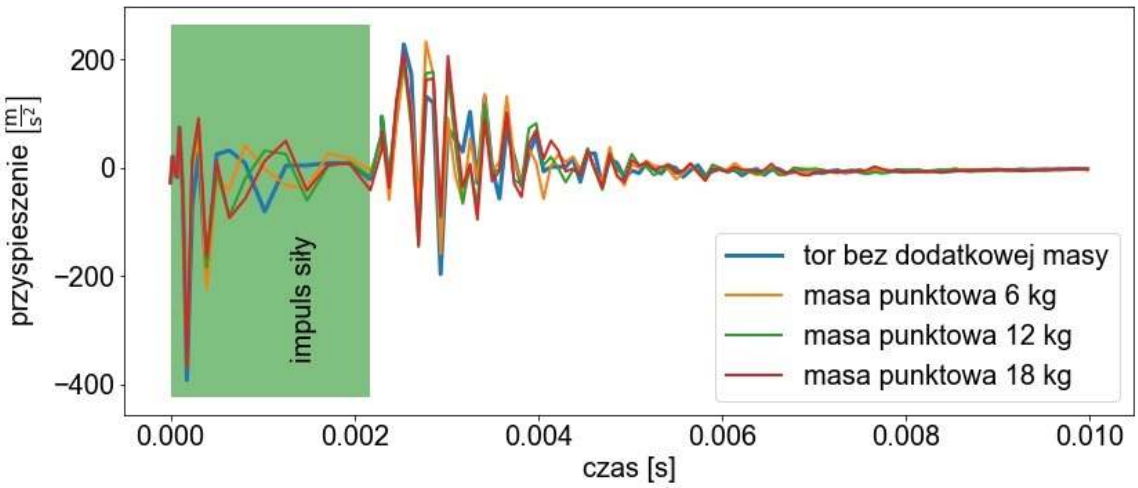

9. Acceleration signal registered at a distance of 0.3 m from the point of load application (above the foundation). Track with 49E1 rail profile

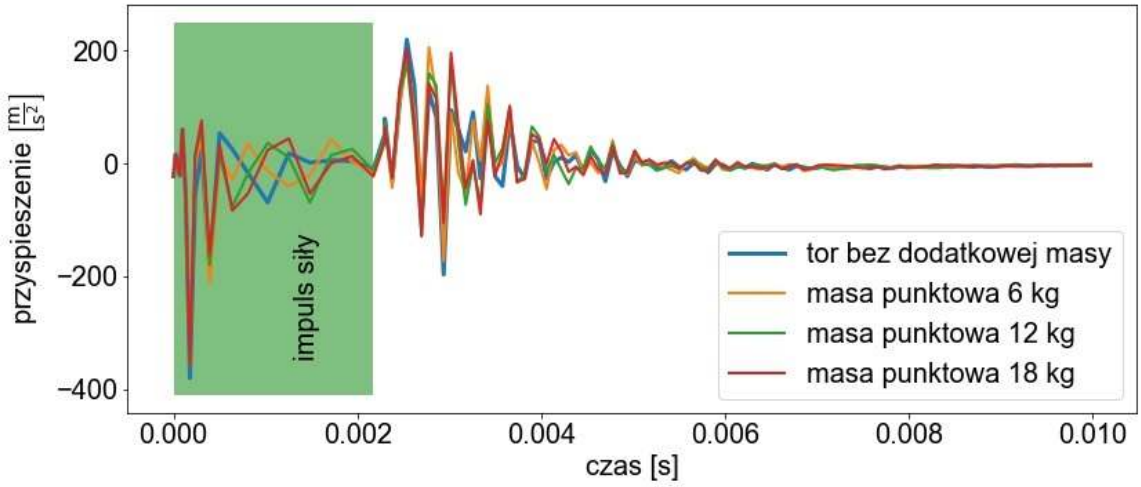

10. Acceleration signal registered at a distance of 0.3 m from the point of load application (above the sleeper). Track with rail profile 60E1

Analogous acceleration diagrams, however, at a distance of 30 cm from the point of load application (above the foundation), are shown in Figures **9** and **10**. Qualitatively, the acceleration plots are similar to those recorded in the middle of the span, however, as to the value, the amplitudes are more than one hundred times smaller. Such a large decay of acceleration is associated not so much with the distance as with the location of the measurement cross-section over the foundation. As can be seen in diagrams **11** and **12**, the amplitude of acceleration is again greater, despite the fact that the distance has increased by another 30 cm.

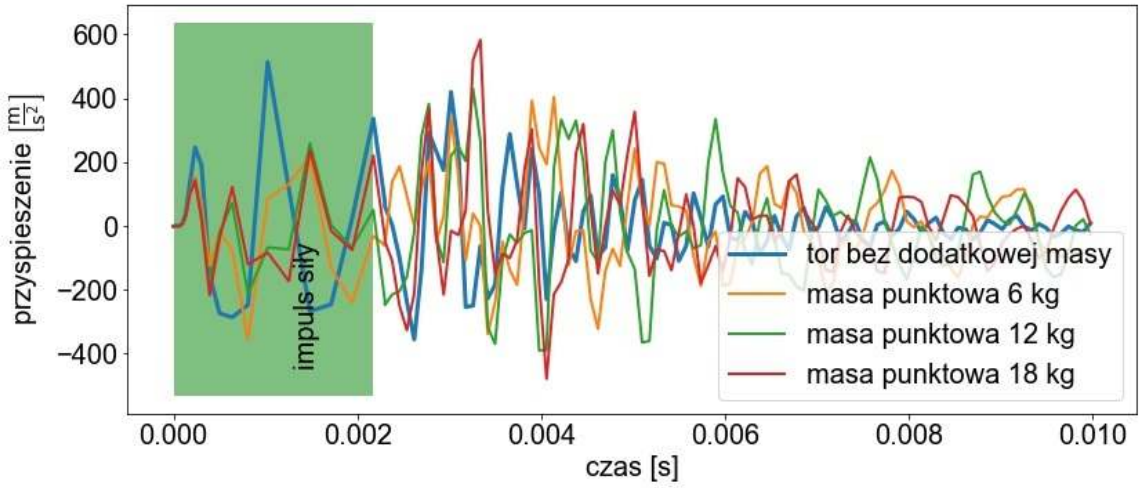

11. Acceleration signal registered at a distance of 0.6 m from the point of load application (in the middle of the span). Track with 49E1 rail profile

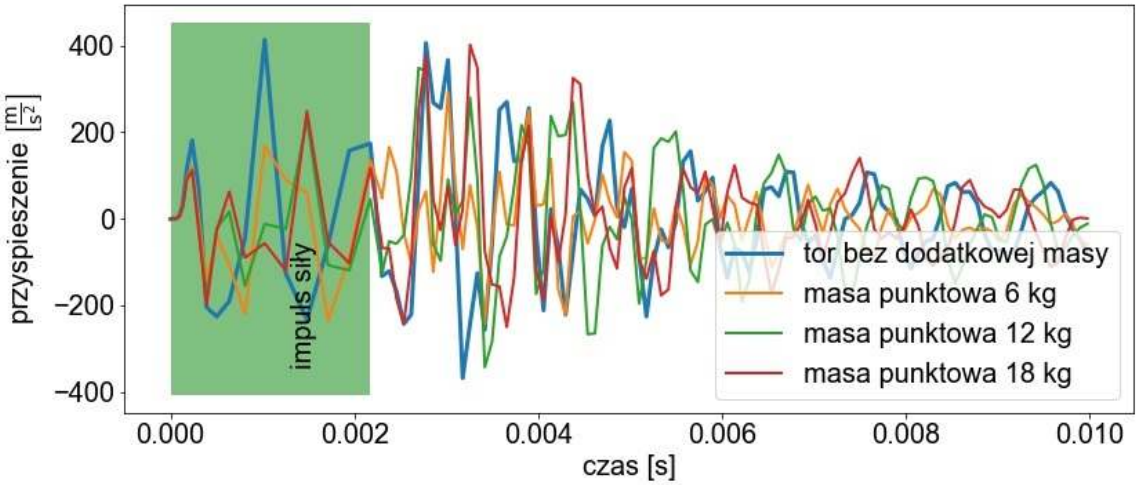

12. Acceleration signal registered at a distance of 0.6 m from the point of load application (in the middle of the span). Track with rail profile 60E1

Supporting the structure in a periodic manner causes that the drop in the amplitude of the acceleration is not a monotonic function at all. The accelerations recorded over the sleepers will stand out from the general trend. The next graphs show the results recorded at a much greater distance, where the construction response appears with a certain delay and the vibrations are no longer so violent. Therefore, the results from a longer time interval are presented.

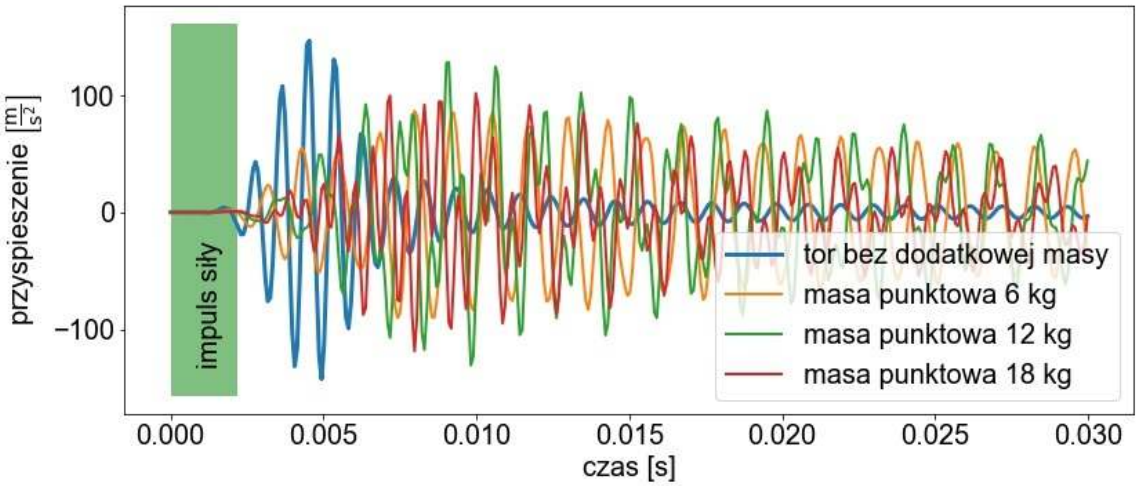

13. Acceleration signal registered at a distance of 3.0 m from the point of load application (in the middle of the span). Track with 49E1 rail profile

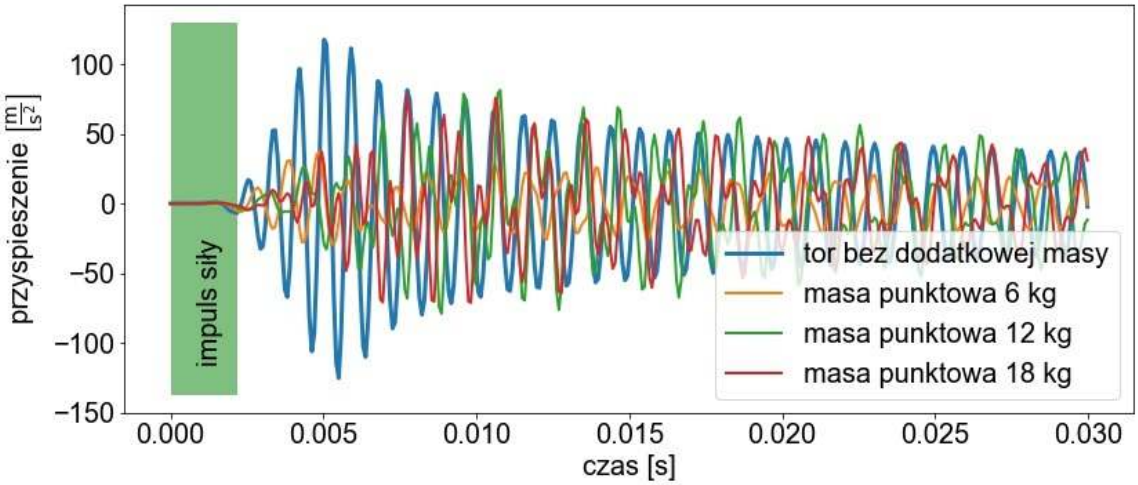

14. Acceleration signal registered at a distance of 3.0 m from the point of load application (in the middle of the span). Track with rail profile 60E1

The response of the structure at a distance of 3.0 m from the point of extortion (Figures **13** and **14**) is already more diverse. In the case of the track with the rail profile 49E1, it can be noticed that track vibrations without additional mass reach maximum earlier and disappear in time much faster than track vibrations with silencers (modeled in the form of a point located mass). However, the use of the 60E1 profile means that track vibrations with an underloaded rail path do not disappear so quickly and for a certain time they remain at a similar level as when using additional weight. It is also worth noting that in the case of both rail profiles one frequency of the acceleration signal is clearly dominant in the track without attenuators, and after their application, the signal is composed.

As the distance increases, the differences become even more apparent. Figures **15** and **16** show the graphs of accelerations recorded at a distance of 18.0 m from the point of extortion.

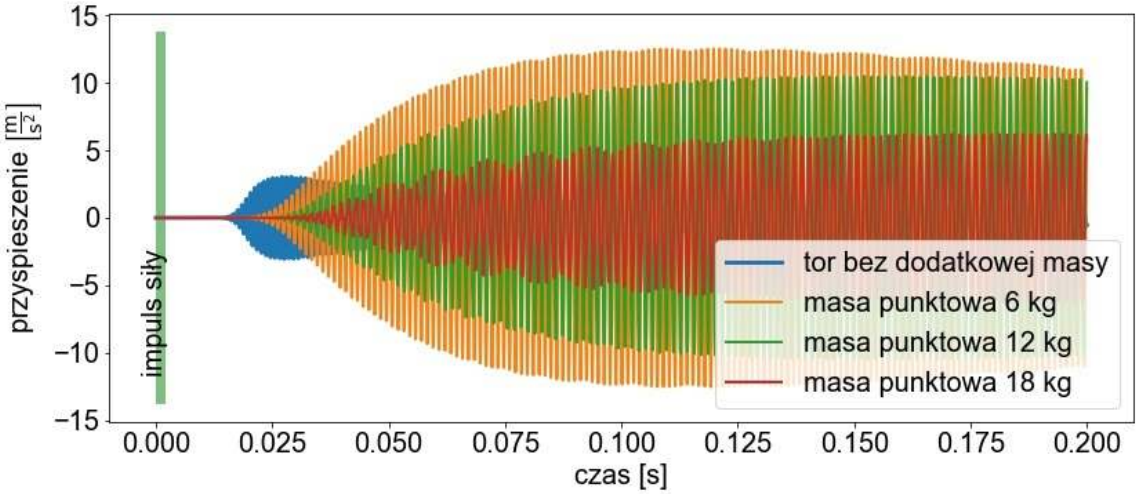

15. Acceleration signal registered at a distance of 18.0 m from the point of load application (in the middle of the span). Track with 49E1 rail profile

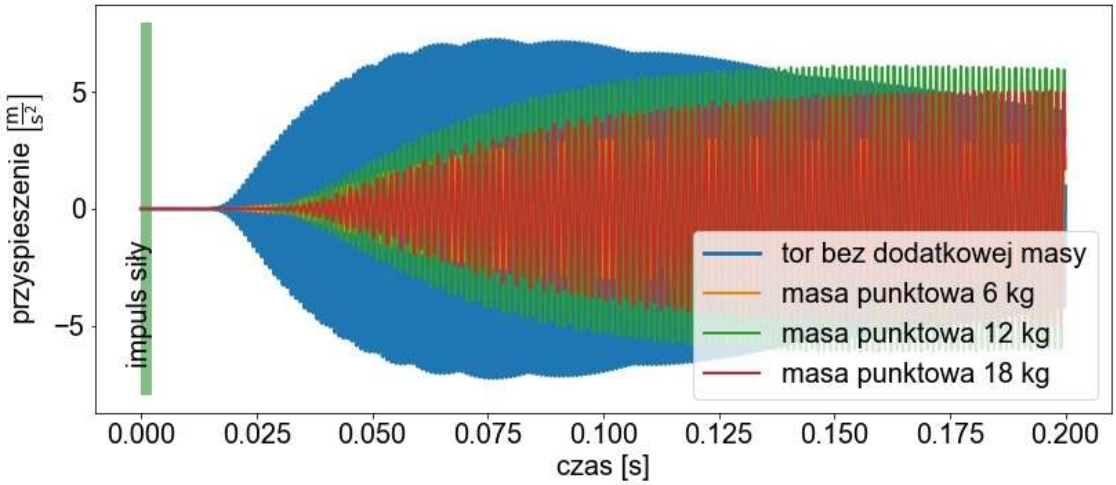

16. Acceleration signal registered at a distance of 18.0 m from the point of load application (in the middle of the span). Track with rail profile 60E1

Analyzing Figure **15**, it can be seen that in a given section the rail course experiences much smaller accelerations if no additional load is applied. On the other hand, the introduction of faders makes the recorded acceleration greater. The biggest one is when adding a weight of 6 kg, and then with increasing load, the acceleration decreases. In the case of the 60E1 rail profile (Figure **16**), the situation is almost the opposite. Maximum accelerations were recorded in the track without dampers while as the mass increased, the amplitude of the acceleration decreases.

As it results from the presented example results, vibrations closer to the point of excitation occur rapidly, with high frequency and amplitude. As we move away from the source of excitation, we can observe not only a change in the amplitude but also a change in the dominant frequency. It can be concluded from this that vibrations of different frequencies, propagating along the rail, disappear at different rates. Therefore, the analysis is carried out by comparing the signals separated into third bands (according to the standard [2] from 100 to 5000 Hz). The results are presented as the RMS ratio of the signal at a given point to the RMS signal at the point of excitation (RMS0). It is a substitute measure to map the ratio of acceleration amplitudes, but easier to determine. Assuming an exponential drop in amplitude, the charts should be arranged in a straight line. Due to some deviations from the assumptions (e.g the structure is not supported uniformly and periodically), the diagrams take on a different shape. Therefore, instead of determining the TDR directly from the slope of the graph, the standard proposes a simplified formula (equation 2), which should be resistant to these deviations. An exemplary vibration decay diagram is shown in Figure **17**.

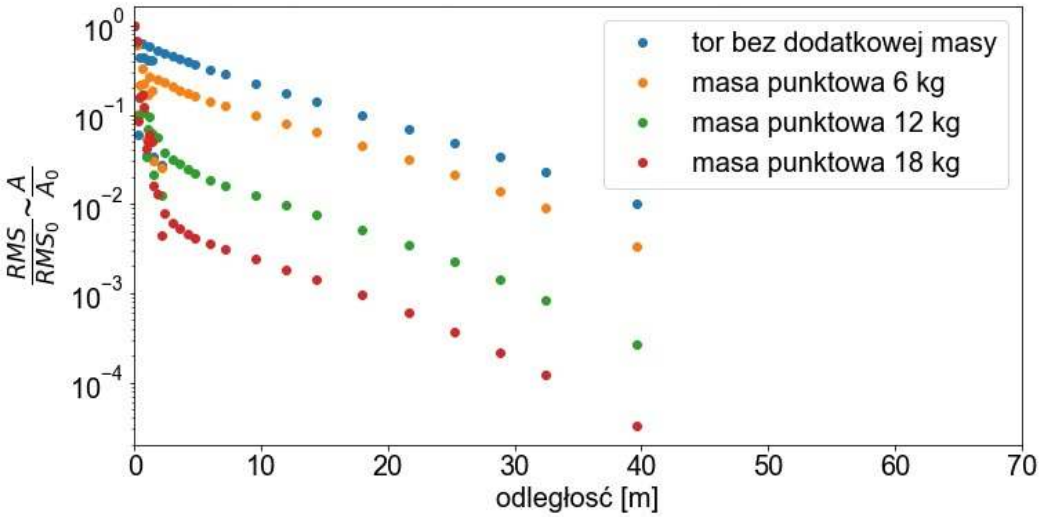

17. Visualization of the vibration decay in the 1000 Hz frequency band (60E1 rail profile)

In the shown graph (Fig. **17**), it can be seen that the higher the added weight, the faster the vibrations disappear along the path (this means a higher value of the TDR parameter). However, in the case of the 630 Hz band (Figure **18**) the situation is reversed.

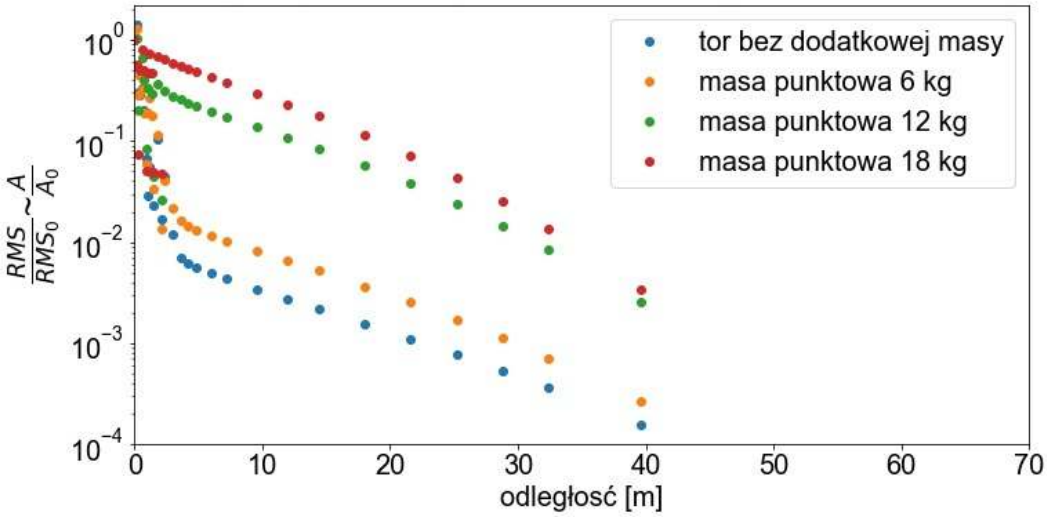

18. Visualization of the vibration decay in the 630 Hz frequency band (rail profile 60E1)

Adding weight makes the situation worse. Probably an increased weight of the track influenced the reduction of the natural frequency of the structure. This is even more visible on the TDR chart (Figure **19**).

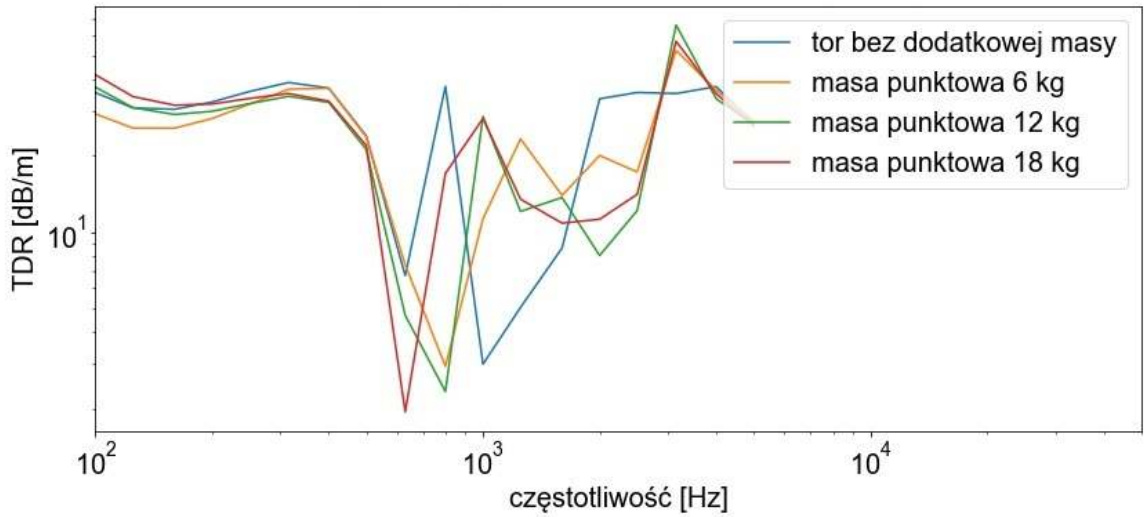

Fig. 19 – Track decay rate (TDR) determined on the basis of the simulation of the test using the finite element method (60E1 rail profile)

When analyzing the graph, it can be noticed that modifying the dynamic characteristics of the track may reduce the emitted noise in some frequencies and increase in others. An analogous effect is shown in Figure **20**, which shows the TDR diagram of the solutions used in the track with the 49E1 rail profile.

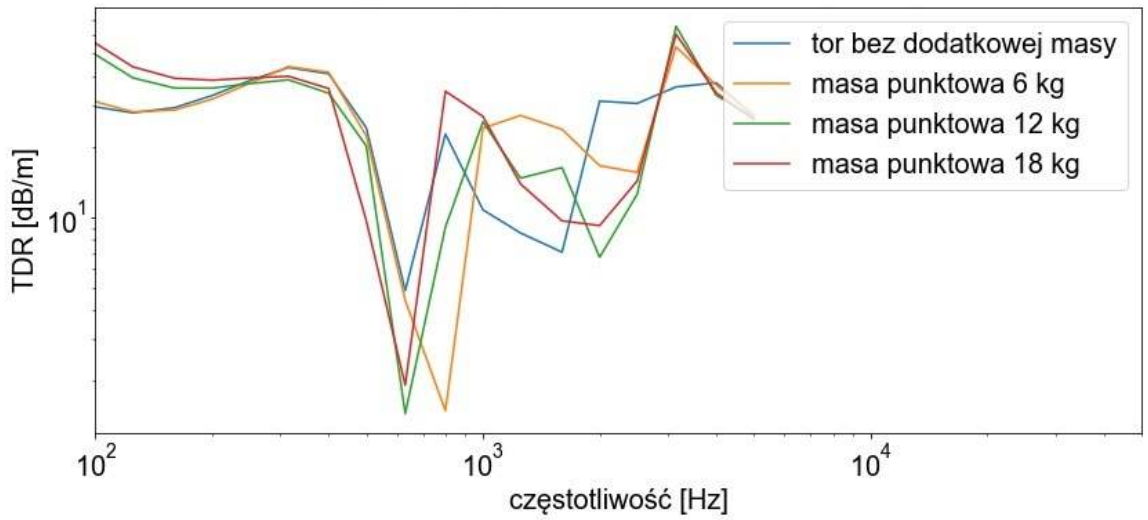

20. Track decay rate (TDR) determined on the basis of the simulation of the test using the finite element method (rail profile 49E1)

In both cases, the vibrations disappear the slowest in the bands between 630 Hz and 800 Hz, with the additional mass transferring this tendency to the lower frequencies. One can not unequivocally answer which of the proposed solutions brings the greatest reduction in noise emission. It is necessary to develop and adopt an optimization criterion in order to select the best solution.

Conclusions

The simulations of the TDR study and the analysis of intermediate results and final results presented in the article allow to draw many valuable conclusions.

- The increase in mass affects ambiguously the limitation of vibrations in the railroad (and thus noise emission) at different frequencies. For example, in the bands from 630 HZ to 800 Hz one should expect higher vibrations when adding the concentrated mass. However, in the 1000-2000 Hz bands, the additional mass influences the increase of TDR, and thus the reduction of noise emission.
- It is necessary to develop an optimization criterion that allows to clearly determine which solution gives the best noise suppression effect.
- The solution consisting only of rigid connection of the mass (e.g. welding of weights), would be unfavorable, and probably even unacceptable due to a significant increase in noise emission in the bands from 630 HZ to 800 Hz. In fact, the dynamic response of the dampers is more complex, so it should be striven for better mapping and development of the FEM model.
- As the presented research methodology develops, it can become a cheap and accurate tool for testing solutions to protect against noise from rail and tram traffic.

Further work will focus on modeling silencers with more complex models. Instead of replacing the dampers with a single concentrated mass rigidly fixed to the rail course, models from a series of viscous-elastic joints will be used. Such a model is more similar to the behavior of real dampers. It allows reflecting the first few natural frequencies of these devices and additional material damping. Finally, the developed methodology will allow you to test the designed devices in the track (in a simulation environment), before the prototype is built.

Information on financing:

The publication was created as part of the project "Innovative solutions in the field of protection of people and the environment against noise from railway traffic". The project is co-financed by the European Union from the European Regional Development Fund under the Intelligent Development Operational Program and by PKP PLK S.A. within the framework of the BRIK Joint Venture

Source materials

[1] Dittrich, M. G., & Janssens, M. H. A. (2000). Improved measurement methods for railway rolling noise. Journal of Sound and Vibration, 231(3), 595-609.
[2] EN 15461:2008+A1 Railway applications - Noise emission - Characterisation of the dynamic properties of track sections for pass by noise measurements
[3] Jones, C. J. C., Thompson, D. J., & Diehl, R. J. (2006). The use of decay rates to analyse the performance of railway track in rolling noise generation. Journal of Sound and Vibration, 293(3-5), 485-495.
[4] Kaewunruen, S., & Remennikov, A. (2008). Dynamic properties of railway track and its components: a state-of-the-art review.
[5] Remington, P. J. (1987). Wheel/rail rolling noise, I: Theoretical analysis. The journal of the Acoustical Society of America, 81(6), 1805-1823.
[6] Remington, P. J. (1988). Wheel/rail rolling noise: What do we know? What don't we know? Where do we go from here?. Journal of Sound and Vibration, 120(2), 203-226.
[7] Thompson, D. J., Hemsworth, B., & Vincent, N. (1996). Experimental validation of the TWINS prediction program for rolling noise, part 1: description of the model and method. Journal of sound and vibration, 193(1), 123-135.

[8] Thompson, D. J., Jones, C. J. C., & Turner, N. (2003). Investigation into the validity of two-dimensional models for sound radiation from waves in rails. The Journal of the Acoustical Society of America, 113(4), 1965-1974.
[9] Thompson, D. J., Jones, C. J. C., Waters, T. P., & Farrington, D. (2007). A tuned damping device for reducing noise from railway track. Applied acoustics, 68(1), 43-57.
[10] Thompson, D. (2008). Railway noise and vibration: mechanisms, modelling and means of control. Elsevier.
[11] Thompson, D. J. (2008). A continuous damped vibration absorber to reduce broad-band wave propagation in beams. Journal of sound and vibration, 311(3-5), 824-842.
[12] Squicciarini, G., Toward, M. G. R., & Thompson, D. J. (2015). Experimental procedures for testing the performance of rail dampers. Journal of Sound and Vibration, 359, 21-39.
[13] Zhang, X., Thompson, D. J., Li, Q., Kostovasilis, D., Toward, M. G., Squicciarini, G., & Ryue, J. (2019). A model of a discretely supported railway track based on a 2.5 D finite element approach. Journal of Sound and Vibration, 438, 153-174.